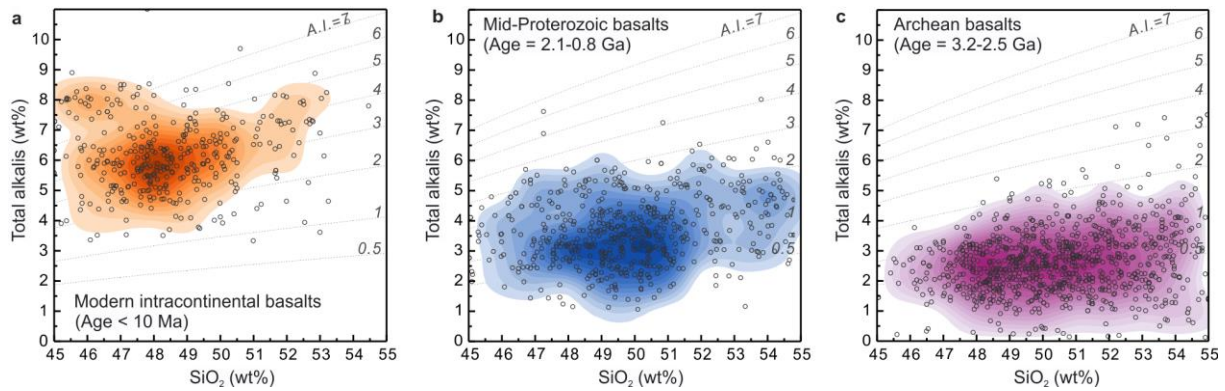
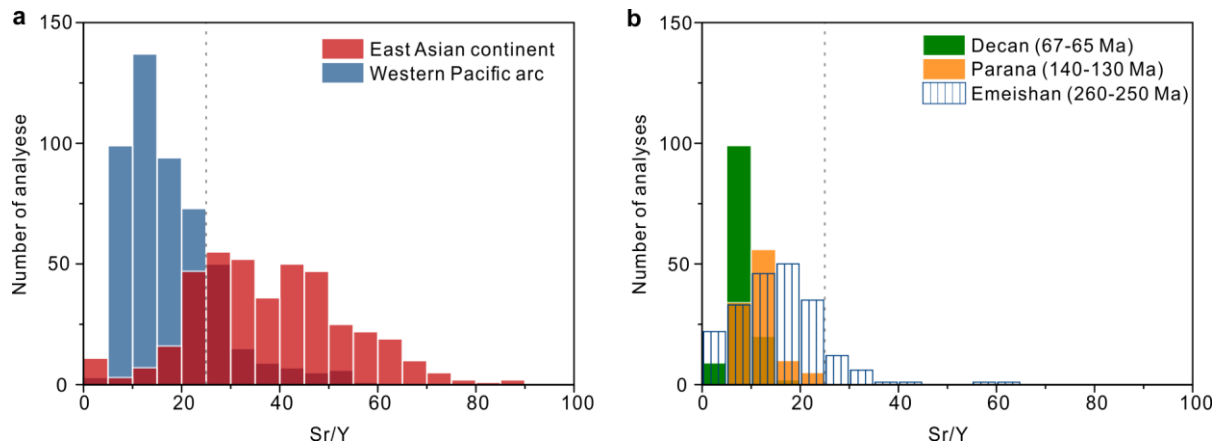


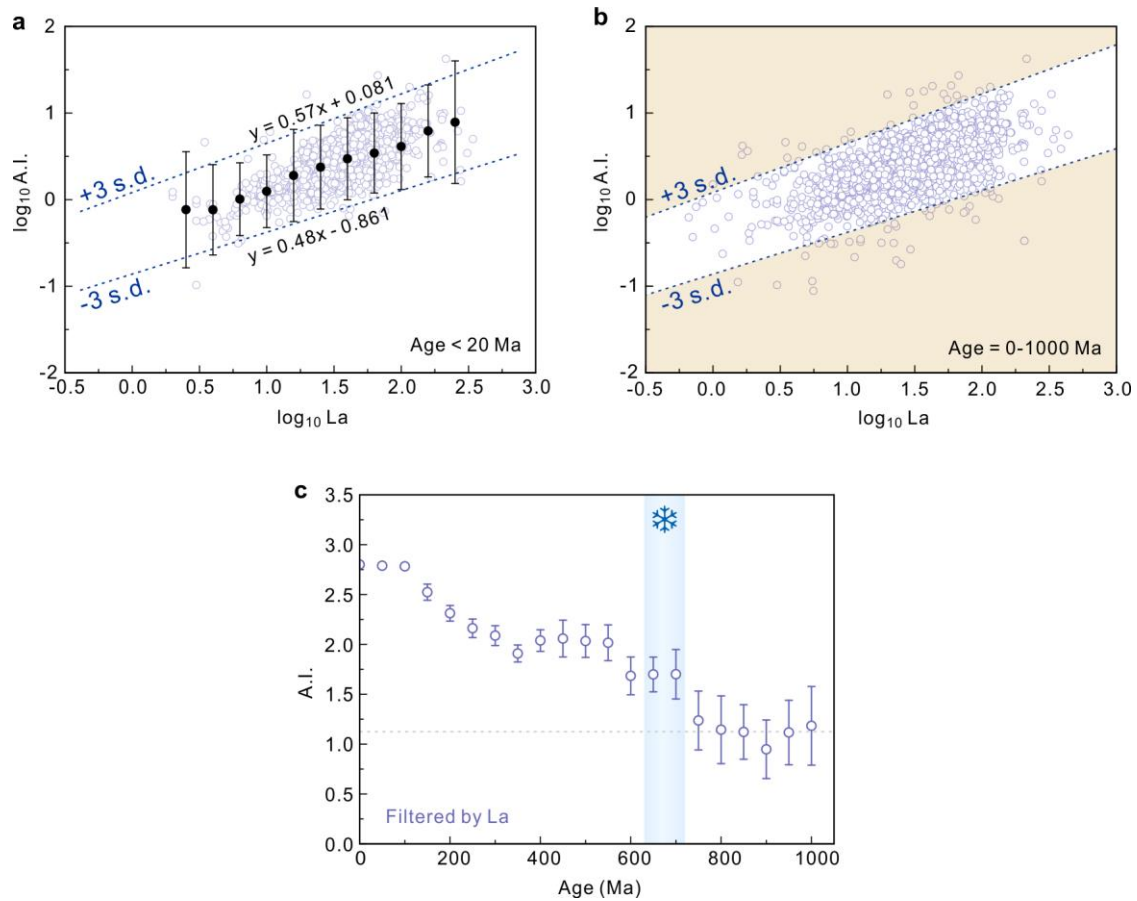
Supplementary Fig. 1 The total alkali vs SiO₂ content of basalts from intracontinental and arc setting. **a.** Plot of the total alkali (Na₂O + K₂O) content in basalts (younger than 10 Ma) from eastern Asia. **b–c.** Scatter plots and density contours of the total alkali vs SiO₂ content of intracontinental and arc basalts, respectively. Data were extracted from the EarthChem database (www.earthchem.org/portal). The background relief map was downloaded from the NOAA website (<https://www.ngdc.noaa.gov/>)¹.



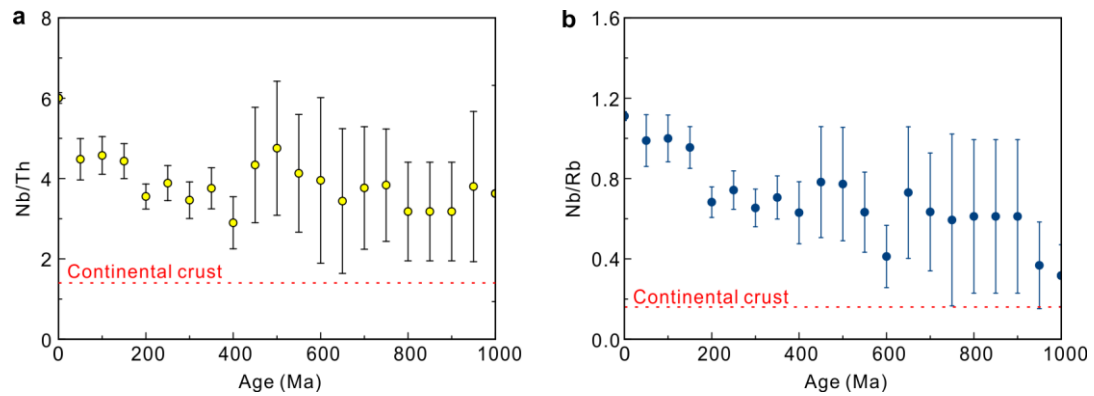
Supplementary Fig. 2 Comparison of the Alkali Index (A.I.) vs silica content in modern intracontinental, mid-Proterozoic, and Archean basalts. Plots and density contours of the total alkali ($\text{Na}_2\text{O} + \text{K}_2\text{O}$) vs SiO_2 content of modern intracontinental basalts (<10 Ma), mid-Proterozoic (2.1–0.8 Ga), and Archean basalts (3.2–2.5 Ga). The locations of the modern intracontinental basalts are shown in Supplementary Fig. 1a.



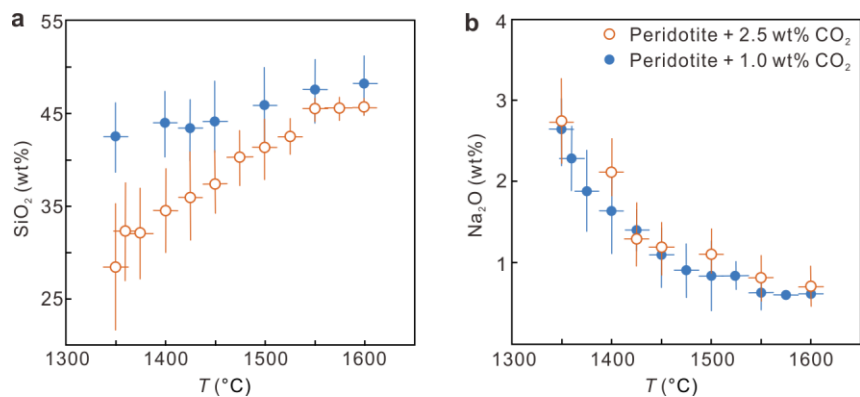
Supplementary Fig. 3 The Sr/Y systematics of intracontinental, arc, and large igneous province basalts. **a.** Histograms showing the Sr/Y ratios of <10 Ma basalts from the East Asian continent and western Pacific arc. Locations of samples are shown in Supplementary Fig. 1a. **b.** Histograms showing the Sr/Y ratio of basalts from the Decan, Parana, and Emeishan large igneous provinces (LIPs). Data were extracted from the EarthChem database (www.earthchem.org/portal). The ages of the samples are shown in the legend. The dashed vertical lines in both figures denote Sr/Y = 25.



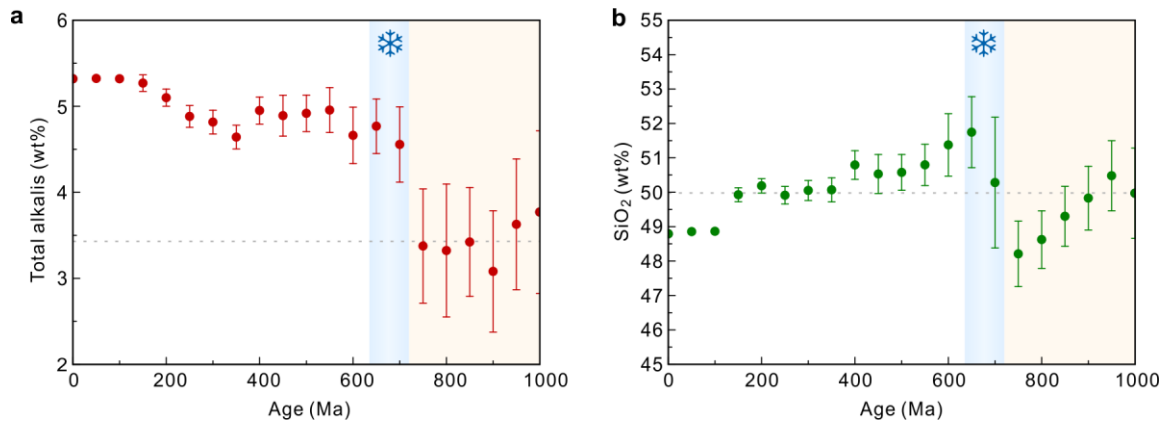
Supplementary Fig. 4 Plots showing the processes of data filtering to minimize the influence of alteration and metamorphism on the intracontinental basalts. **a.** Plot of \log_{10} A.I. vs \log_{10} La for < 10 Ma basalts. **b.** The plot of \log_{10} A.I. vs \log_{10} La for all intracontinental basalts. The data within the areas covered by the yellow polygons were removed prior to performing the statistical analysis. **c.** Secular variations in A.I. for the La-filtered data.



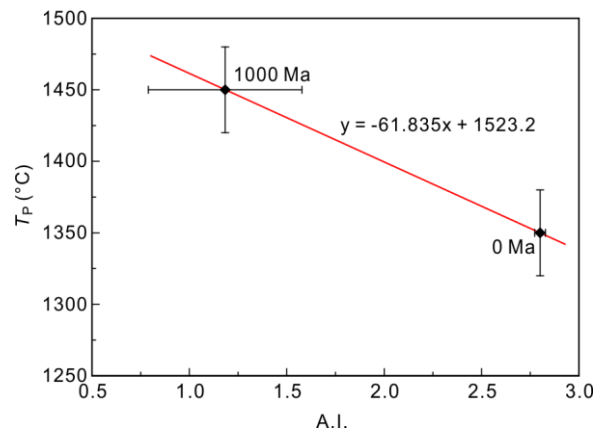
Supplementary Fig. 5 Secular variations in Nb/Th and Nb/Rb ratios in intracontinental basalts since the Neoproterozoic (1000–0 Ma). a. Secular variation in Nb/Th. **b.** Secular variation in Nb/Rb. The horizontal red dashed lines show the Nb/Th or Nb/Rb ratios of the bulk continental crust (from ref. ²).



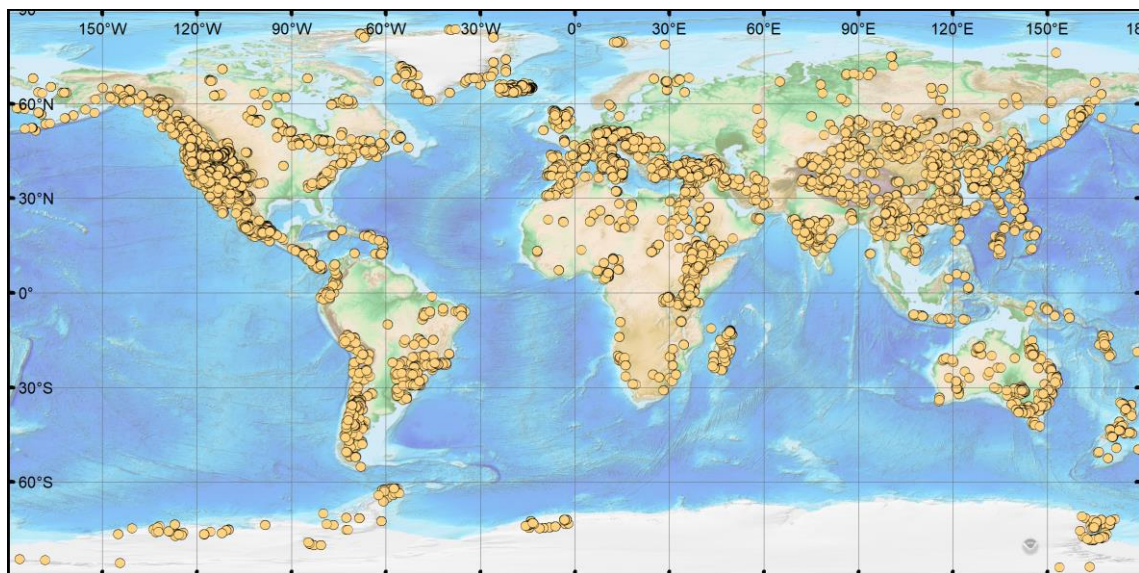
Supplementary Fig. 6 Composition of carbonate-bearing silicate partial melts from PERC (peridotite + 2.5 wt% CO₂) and PERC3 (peridotite + 1.0 wt% CO₂) carbonated peridotite partial melting experiments at 3 GPa (modified from ref³). **a.** SiO₂ content in the melt from partial melting of PERC and PERC3. **b.** Na₂O content in the melt from the partial melting of PERC and PERC3. The increase of CO₂ in the mantle source leads to a decrease in the SiO₂ content of the melt but has almost no effect on Na₂O content.



Supplementary Fig. 7 Secular variations in the total alkalis and silica content of intracontinental basalts since the Neoproterozoic (1000–0 Ma). The intracontinental basalts are filtered by $\text{Sr/Y} > 25$ as they are mostly generated by high-pressure melting (Supplementary Fig. 3). **a–b.** Secular variations in total alkali ($\text{Na}_2\text{O} + \text{K}_2\text{O}$) content and SiO_2 content, respectively. The moving average has a 200-Myr window. Error bars denote two standard errors on the means (s.e.m.). The light-blue vertical columns with a snowflake symbol represent the Cryogenian Snowball Earth event at ~ 720 – 635 Ma⁴. The grey horizontal dashed lines show the average values before the Cryogenian.



Supplementary Fig. 8 Comparison between the alkali index (A.I.) and previously proposed mantle potential temperature (T_P). We compare the data in the previous T_P model at 1000 and 0 Ma with the average A.I. in contemporaneous intracontinental basalts.



Supplementary Fig. 9 Spatial distribution of all basaltic rocks (45–55 wt% SiO₂) used in this study (*n* = 43,836). The data were downloaded from the EarthChem database with appropriate filtering. The background relief map was downloaded from the NOAA website (<https://www.ngdc.noaa.gov/>)¹.

References

- 1 Amante, C. & Eakins, B. W. ETOPO1 arc-minute Global Relief Model: Procedures, Data Sources And Analysis. NOAA Technical Memorandum. Report No. NESDIS NGDC-24, 1–19 (National Geophysical Data Center, NOAA, Boulder, Colorado, 2009).
- 2 Rudnick, R. L. & Gao, S. in *Treatise on Geochemistry (Second Edition)* (eds Heinrich D. Holland & Karl K. Turekian) 1–51 (Elsevier, 2014).
- 3 Dasgupta, R., Hirschmann, M. M. & Smith, N. D. Partial Melting Experiments of Peridotite + CO₂ at 3 GPa and Genesis of Alkalic Ocean Island Basalts. *J Petrol* **48**, 2093–2124, doi:10.1093/petrology/egm053 %J Journal of Petrology (2007).
- 4 Hoffman, P. F., Kaufman, A. J., Halverson, G. P. & Schrag, D. P. A Neoproterozoic Snowball Earth. *Science* **281**, 1342, doi:10.1126/science.281.5381.1342 (1998).